Electrical resistivities of γ-phase $Fe_xNi_{80-x}Cr_{20}$ alloys

S. Banerjee and A. K. Raychaudhuri
Department of Physics, Indian Institute of Science, Bangalore 560012, India
(Received 17 February 1994)

In this paper we present a comprehensive investigation of electrical resistivities [$\rho(T)$] of the γ-phase pseudobinary Fe alloy series $Fe_xNi_{80-x}Cr_{20}$ in the temperature range 0.4–300 K. These alloys exhibit exotic magnetic behavior at and near the critical composition for ferromagnetism $x_c \simeq 59$–63. Special attention has been given to the critical region ($x \simeq x_c$) where we find sharp changes in ρ_0 (zero temperature resistivity) as well as in the temperature dependence of $\rho(T)$. These observations have been explained as arising due to the absence of long-range magnetic order and a change in effective carrier concentration at $x \simeq x_c$. For all $x(\leq 66)$ these alloys exhibit a resistivity minimum at $T = T_{min}$. T_{min} continuously decreases from approximately 35 K for $x \approx 12$ to approximately 6 K for $x \approx 59$. $\rho(T)$ for $T < T_{min}$ shows a rise ($\rho \sim -\sqrt{T}$) that does not depend on the magnetic state of the alloy. For $T_{min} < T < 80$ K, $\rho(T)$ away from x_c follows a predominantly T^2 dependence arising from electron–spin-wave scattering which shows a drastic reduction for $x \approx x_c$. We also compare our data with an α-phase $Fe_{25}Cr_{75}$ alloy.

I. INTRODUCTION

In alloys containing high concentrations of magnetic metals (such as 3*d* metals), the interpretation of electronic transport properties has always been difficult and controversial. A detailed quantitative understanding of these properties has not yet been achieved, although much qualitative knowledge has been obtained through transport studies. Most of these alloys have high electrical resistivities. Rapid expansion of this subject has led to intensive and extensive investigations on amorphous metals such as metallic glasses.[1] However, not much attention has been paid lately to highly resistive crystalline alloys. It is our purpose here to show that transport properties of these alloys are interesting in their own right, and that they pose considerable challenges in understanding them. Many of these alloys can also have exotic magnetic phases, and one encounters an interplay of electronic and magnetic properties. It is known that the addition of transition metals and lattice disorder increases the ρ of an alloy. The point we would like to stress is that even in substitutionally disordered transition-metal polycrystalline alloys, one can obtain a ρ which is similar to or even higher than the ρ seen in nontransition-metal amorphous alloys. The transition-metal-based amorphous alloys have a ρ much higher than the rest. In this investigation we studied the electrical transport properties of highly resistive polycrystalline alloys with special reference to γ-phase Fe-Ni-Cr alloys. The γ-phase Fe-Ni-Cr alloys in the Fe-rich end form stainless-steel alloys which are weakly antiferromagnetic or nonmagnetic. In the Ni-rich end they show ferromagnetism.

The choice of this particular γ-phase Fe-Ni-Cr alloy series has been made on the following considerations.

(a) The magnetic phase diagram of this alloy series is rather exotic and has been studied extensively in the recent years.[2,3] The magnetic phase diagram is shown in Fig. 1.

(b) Although there exist studies of electrical transport properties of some alloys belonging to this series,[4,5] there are no careful studies of alloys with a composition range around the critical composition for ferromagnetism.

(c) In previous studies of crystalline alloys of this type, the low-temperature range was only down to 4.2 K.[4,5] In this work we report data to a much lower temperature ($T \geq 0.4$ K), which allows us to study the origin of resistivity minima observed in these alloys. A preliminary report about resistivity minima in these alloys has been published before.[6]

(d) By combining our studies with previous work,[4] we can present a complete study of electrical resistivities ρ for the pseudobinary alloys $(Fe_xNi_{80-x})Cr_{20}$ for $7 \leq x \leq 66$, and can study the evolution of ρ as we go from Ni-rich end to the Fe-rich end.

The values of transition temperatures T_c, T_{SG}, and T_N, and saturation magnetization $4\pi M_s$, for these alloys are given in Table I. From the phase diagram of the pseudobinary series (Fig. 1), one finds that in this alloy system by varying x one can go from long-range ordered ferromagnetic (FM) to antiferromagnetic (AFM) via a critical region for $59 \leq x \leq 63$, where one finds a collapse

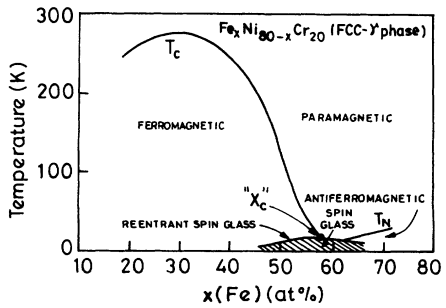

FIG. 1. Magnetic-phase diagram of the pseudobinary (γ-Fe) series $Fe_xNi_{80-x}Cr_{20}$ data obtained from Refs. 2 and 3.

TABLE I. Values of transition temperatures T_c, T_{SG}, and T_N, and saturation magnetization $4\pi M_s$, in $Fe_xNi_{80-x}Cr_{20}$ ($50 \le x \le 66$) alloys (Ref. 2).

Fe%	T_c (K)	T_{SG} (K)	T_N (K)	$4\pi M_s$ (kG)
50	114			3.8
54	56	7		1.92
55	47.5	11.5		0.69
59		10		
60		11		
63			13	
66			26	

of FM order and the onset of AFM order. There are two distinct regions of disordered magnetism in this alloy series. For $x < 12$ one is in the paramagnetic (PM) phase. With increasing x, one sees the onset of ferromagnetism, but a reenterant spin glass (RSG) phase exists for $12 < x < 35$.[3] Only for $x > 35$ does one see stable ferromagnetism. However, for $x > 50$ the ferromagnetism starts collapsing. It passes through a critical region (showing RSG and SG phases), and then with further increase of Fe enters an AFM phase. These are γ-phase fcc alloys with Fe providing the antiferromagnetic interaction[2,3] (note that in this material pair exchange integrals for Fe-Fe and Cr-Cr are antiferromagnetic, whereas other exchange integrals are all ferromagnetic). We also would like to point out that $Fe_xNi_{80-x}Cr_{20}$ is one of few such series where the crystallographic structure remains unchanged while the series undergo a gradual change from one long-range ordered phase (FM) to the other long-range ordered phase (AFM). A similar situation also occurs in the Fe-Ni-Mn system.[7] In contrast, in the binary series Fe_xNi_{100-x} one has the γ phase for $x \le 65$, and goes to the α phase for higher iron concentrations.[8] Addition of Cr stabilizes the γ phase to a higher relative iron concentration and (as shown below) gives these alloys a high value of ρ. In $Fe_xNi_{80-x}Cr_{20}$ the α phase appears for $x \ge 66$. It should also be pointed out that one sees invar (or elinvar) behavior in this composition range.[7]

In this paper we seek answers to the following questions.

(a) What causes high resistivity in these alloys?

(b) What happens to the electrical transport properties at low temperatures in crystalline alloys with concentrated magnetic constituents when we are not in the Kondo regime? (For most Kondo systems the transition-metal composition is much less compared to the percolation threshold.)

(c) What is the role of magnetic order (if any) in electronic transport in alloys which lie close to the critical composition for ferromagnetism, in particular when ones passes through a disordered magnetic phase (like a spin-glass phase)?

(d) What happens to the electron-magnon scattering near the critical region where the spin wave becomes overdamped?

(e) What are the differences in low-temperature electronic transport in γ-phase and α-phase iron alloys? (The α-phase alloy $Fe_{25}Cr_{75}$ studied by us in this paper also sits very close to the critical composition for ferromagnetism, like alloys of Fe-Ni-Cr series.)

(f) Can the concepts of quantum interference be applied to explain low-temperature resistivities of these alloys below the temperature of resistivity minima which we observe in these alloys?

The remaining part of the paper has three sections. In Sec. II we briefly describe the experimental details. In Sec. III we present data and a general discussion. In Sec. IV we discuss the compositional dependence of various parameters obtained from the analysis of the data, and then summarize the answers to the above questions.

II. EXPERIMENTAL TECHNIQUES

The series $Fe_xNi_{80-x}Cr_{20}$, with $x = 50$, 54, 55, 59, 60, 63, and 66, were prepared in ingot form in an arc furnace. These alloys were further annealed for homogeneity at 1050 °C for 100 h in an Ar atmosphere, and then quenched to room temperature to retain the γ phase. An α-phase $Fe_{25}Cr_{75}$ alloy was prepared and heat treated in a similar fashion. All these alloys were characterized by energy dispersive x-ray analysis (EDAX) and chemical analysis to determine the composition. X-ray analysis exhibited Fe-Ni-Cr alloys to be in the fcc γ phase, whereas Fe-Cr are in the α phase. For resistivity measurement, thin strips were obtained by cold rolling, and were further annealed at 1100 °C in an argon atmosphere and quenched in water. (Some of the alloys used here were obtained from Professor A. K. Majumdar, and were used by him in magnetic studies reported in Ref. 2.) Samples used for transport measurement were 0.1–0.2 mm thick, 1–1.5 mm in width, and 2 cm in length. Electrical resistivity $\rho(T)$ was measured in the temperature range 0.4–300 K using a combination of He^3 cryostat and a bath-type cryostat. The resistance was measured using a high precision four-probe ac bridge (20 Hz) with a PC/AT-based automatic data-acquisition program.[9] The schematic circuit diagram of the four-probe ac (20 Hz) bridge is shown in Fig. 2. The basic principle of the bridge is to make the same current pass through the sample (R_s) and a standard resistance (R_{std}). For metallic samples R_s is approximately few tens of mΩ. The voltage developed across it is amplified (typically 100 times) by

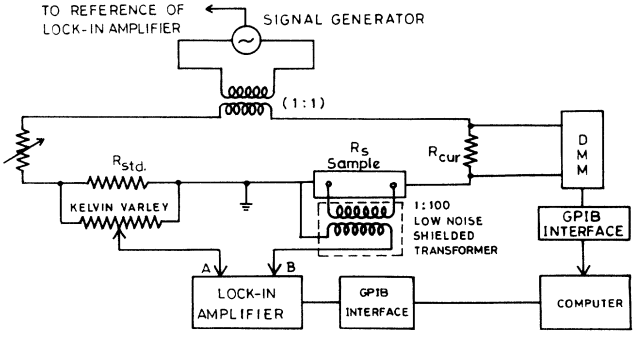

FIG. 2. The circuit used for low noise resistivity measurement at 20 Hz. See text for details.

the low-noise transformer, and balanced against a fraction of the voltage developed across the standard using a Kelvin-Varley voltage divider. Generally at the beginning of the run the lock-in amplifier is nulled by adjusting the Kelvin-Varley voltage divider, which selects the fraction of the voltage developed across the standard for balancing. During the run the off-balance voltage ΔV is measured as a function of temperature using the computer. The voltage at the input of the lock-in is

$$V_A - V_B = IR_{\text{std}} f - IR_s G \ , \tag{1}$$

where R_{std} is the standard resistance, f is the fraction of the voltage obtained from Kelvin-Varley, and G is the gain from the transformer (1:100 low-noise shielded). The current is simultaneously monitored by measuring voltage across the resistance R_{cur}. We used a typical measuring current of 1 mA (rms) to avoid any heating effect. The typical resistance values were around 50 mΩ. The precision of the measurement is around ± 20 ppm. Electrical contacts to samples were made by silver paste or by spring-loaded gold-coated pins. Samples were fixed to the cold finger of the cryostat using Apiezon N grease. The absolute resistance measurement has an error of $\simeq 2\%$ due to finite contact size and the error in measuring the dimensions of the sample.

III. EXPERIMENTAL DATA

The temperature dependence of resistivities $\rho(T)$ in the temperature range 0.4–300 K for $Fe_xNi_{80-x}Cr_{20}$ ($66 \geq x \geq 50$) are shown in Fig. 3. Values of $\rho(T)$ below 20 K are shown in Fig. 4, with T in a logarithmic scale to enhance the low-temperature behavior. We show values of $\rho(T)$ for the α-Fe alloy $Fe_{25}Cr_{75}$ in Fig. 5. For the $Fe_{25}Cr_{75}$ alloy the data for $T < 20$ K are shown in Fig. 5 as an inset. The contrast in the behavior of the two alloys can be seen. All Fe-Ni-Cr alloys exhibit resistivity minima at low temperatures. For the alloys studied by us

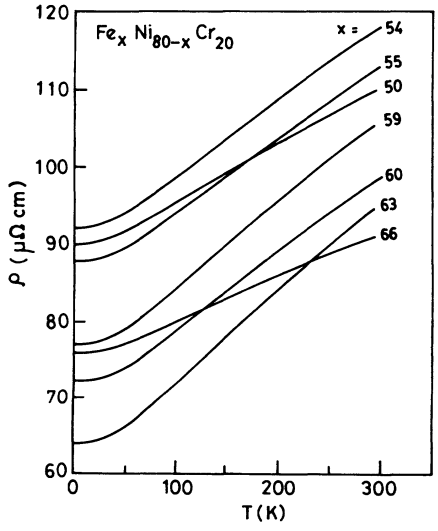

FIG. 3. Resistivities $\rho(T)$ of alloys belonging to $Fe_xNi_{80-x}Cr_{20}$ series.

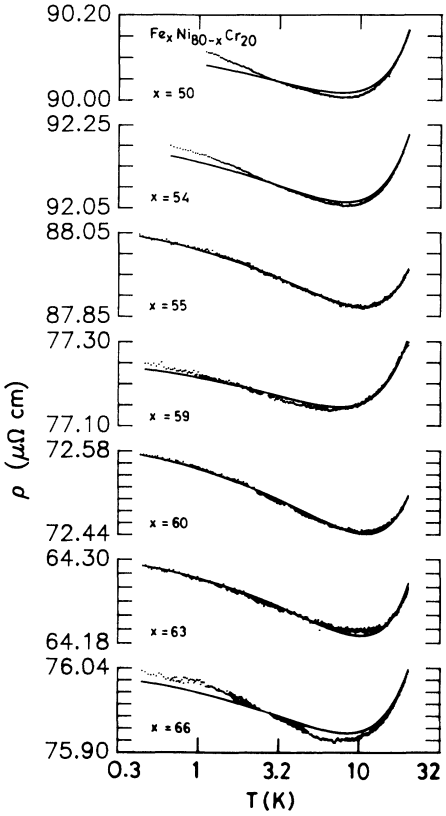

FIG. 4. $\rho(T)$ for $T < 20$ K, shown in an expanded scale to show the occurrence of resistivity minima. The lines are fit to Eqs. (4) and (7). Note that the temperature is shown in a log scale.

$T_{\text{min}} \approx 6$–11 K. It is interesting to note that $Fe_{25}Cr_{75}$ shows no resistivity minimum down to 0.4 K. T_{min} if it occurs at all for this alloy, will be much less than 0.4 K. The temperature-dependent term in $Fe_{25}Cr_{75}$ ($\Delta\rho = \rho_{300\text{ K}} - \rho_0$; ρ_0 is the residual resistivity) is about 53 $\mu\Omega$ cm. This is of the same order as ρ_0, and $\Delta\rho$ in this alloy is much larger than the highest value of $\Delta\rho = 30$ $\mu\Omega$

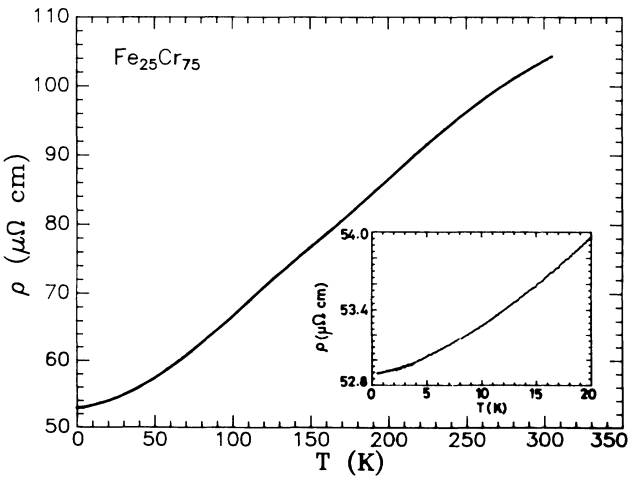

FIG. 5. $\rho(T)$ for $Fe_{25}Cr_{75}$ alloy. The inset shows the data for $T < 20$ K. Note the absence of resistivity minima.

TABLE II. Values of ρ_0, $\rho_{0.4\,K}$, ρ_{min}, $\rho_{300\,K}$, $\Delta\rho(=\rho_{300\,K}-\rho_{min})$, and T_{min} in $Fe_xNi_{80-x}Cr_{20}$ $(50\le x\le 66)$ alloys.

Fe%	ρ_0 ($\mu\Omega$ cm)	$\rho_{0.4\,K}$ ($\mu\Omega$ cm)	ρ_{min} ($\mu\Omega$ cm)	$\rho_{300\,K}$ ($\mu\Omega$ cm	$\Delta\rho$ ($\mu\Omega$ cm	T_{min} (K)
50	90.15	90.15	90.00	109.85	19.85	8
54	92.24	92.22	92.05	118.03	25.98	7.9
55	88.10	88.05	87.87	112.85	24.98	9.2
59	77.28	77.25	77.13	105.51	28.38	6.5
60	72.62	72.58	72.44	98.29	25.85	10.3
63	64.32	64.29	64.20	94.26	30.06	10.5
66	76.06	76.04	75.91	90.94	15.03	7
$Fe_{25}Cr_{75}$		52.89		104.37	51.48	

cm observed in the Fe-Ni-Cr series. We will discuss the $Fe_{25}Cr_{75}$ alloy below.

In Table II, for all the Fe-Ni-Cr alloys studied by us, we show the values of resistivities at 0.4 K ($\rho_{0.4\,K}$), at $T=T_{min}(\rho_{min})$ at room temperature ($\rho_{300\,K}$), and change in resistivities $\Delta\rho$ ($\Delta\rho=\rho_{300\,K}-\rho_{min}$). We also show the extrapolated zero-temperature resistivity ρ_0. The procedure for obtaining ρ_0 will be discussed below. The difference between ρ_0 and ρ_{min} is less than 0.2%. The values of T_{min}, $\rho_{300\,K}$, ρ_0 and $\Delta\rho$ as functions of Fe concentration are shown in Fig. 6 along with data from Ref. 4. A detailed analysis of Fig. 6 will be done in Sec. IV. One can see that the electronic transport in this alloy series shows a rather interesting behavior when x is changed. The most spectacular behavior occurs as one approaches the critical region for $x\simeq 60-63$.

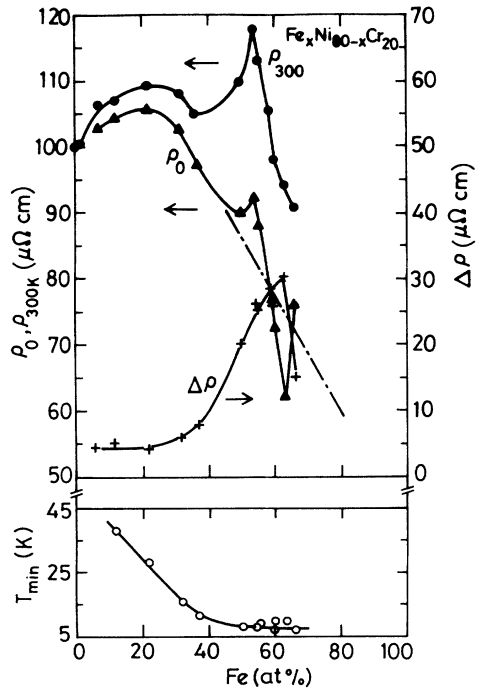

FIG. 6. ρ_0, $\rho_{300\,K}$, $\Delta\rho$ $(=\rho_{300\,K}-\rho_{min})$, and T_{min} as functions of x. The data for $x<37$ have been obtained from Ref. 4. The dash-dotted line gives the expected variation of ρ_o in the absence of the anomaly at the critical region $x\approx 59-63$ (See text).

In the rest of this section we explore the quantitative details of the data. First we present and discuss the temperature dependence of resistivity $\rho(T)$ for $T\ge T_{min}$ including the region close to T_{min} for the Fe-Ni-Cr alloys. Next we discuss our data for $T\ll T_{min}$. After that we compare our data for the Fe-Ni-Cr system with the Fe-Cr system.

A. Region above and close to resistivity minima ($T\ge T_{min}$)

The $\rho(T)$'s for a wide variety of metallic alloys (especially the highly resistive ones) generally vary as T^2 at low temperatures ($T\le 80$ K) and show almost linear temperature dependence at high temperatures ($T\ge 100$ K). For many crystalline alloys or compounds with high resistivities ($\rho\ge 100$ $\mu\Omega$ cm) the $\rho(T)$'s show a trend toward saturation beyond the linear region. (Examples are A-15 compounds such as Nb_3Sn and V_3Ge.[10,11])

For our system for $T>100$ K, $\rho(T)$ approximately follows a linear relation as

$$\rho(T)=\rho_c+A_1T\ . \tag{2}$$

This linear behavior, as in other metallic alloys, arises from electron-phonon interaction. In Table III we show ρ_c and A_1 for all alloys. In Fig. 7 we show the $d\rho/dT$ for three Fe-Ni-Cr alloys studied by us as representative examples. Three important observations can be made from this. First, above 150 K $d\rho/dT$ is nearly constant (within 10%). But alloys with x close to x_c show a gradual decrease. Though in these alloys ρ can be as high as 120 $\mu\Omega$ cm, we do not see any sign of resistivity saturation ($d\rho/dT\to 0$) at 300 K. However, if $\rho(T)$ continues to rise quickly, an approach to resistivity saturation for $T>400$ K and $\rho(T)>150$ $\mu\Omega$ cm cannot be ruled out. Second, there is a distinct change in slope below 100 K with $d\rho/dT$ varying almost linearly with T below 50 K. Third, $d\rho/dT$ does not show any feature at magnetic transitions, and we do not see any critical behavior at T_c in $d\rho/dT$.

In the temperature range $T_{min}<T<80$ K, the variation of $\rho(T)$ needs special attention. In conventional Bloch-Grüneisen theory (for electron-phonon interaction) it is expected that $\rho(T)$ will approach the residual resistivity with a T^5 dependence. A T^3 dependence is expect-

TABLE III. The fit parameters ρ_c, A_1, A_2, A_3, and a_ρ.

Fe%	ρ_c ($\mu\Omega$ cm)	$A_1(10^{-2}$ $\mu\Omega$ cm/K)	$A_2(10^{-4}$ $\mu\Omega$ cm/K^2)	$A_3(10^{-6}$ $\mu\Omega$ cm/K^3)	$a_\rho(10^{-1}$ ($\mu\Omega$ cm)/$\sqrt{\text{K}}$
2	97.8	0.85			
7	101.5	1.85			
12	102.5	1.65	1.42		16.91
22	104.3	2.00	1.74		13.96
32	100.8	2.60	2.66		9.72
37	96.0	3.25	3.06		8.59
50	87.9	7.50	7.20	0.255	6.18
54	89.1	9.80	8.83	0.137	8.27
55	84.4	9.59	7.14	0.186	9.56
59	73.4	11.03	7.58	2.574	6.49
60	68.8	10.03	4.11	4.756	7.10
63	60.4	11.74	3.04	7.936	5.57
66	74.2	5.70	5.86	0.126	5.67

ed for electron-phonon interaction in the presence of s-d scattering. For alloys of this type a T^3 dependence is more likely. This temperature dependence (T^3 or T^5) is caused by the electron-phonon interaction, which manifests at higher temperature as a linear temperature dependence. In addition, we can have a T^2 contribution to $\rho(T)$ originating from either electron-electron or electron-magnon scattering. Our attempt will be made to see if we can detect the presence of these terms in $\rho(T)$. The problem is further compounded by the fact that we have a resistivity minima, and there is a small but distinct rise of $\rho(T)$ for $T<T_{\min}$. It is important to take into account the fact that whatever causes the rise in $\rho(T)$ below $T_{\min}$ will also be present for $T\geq T_{\min}$, at least for some temperature range. However, the contribution of this term to $\rho(T)$ becomes progressively negligible as T is raised well above $T_{\min}$. To make our work managable, here we have to use the result of Sec. III B in advance. We will show in there that the rise in $\rho(T)$ well below $T_{\min}$ follows the relation

$$\rho(T)=\rho_o-a_\rho\sqrt{T}\ ,\quad T\ll T_{\min}\ , \tag{3}$$

where ρ_o is the resistivity at $T=0$ K. In our model, the resistivity minima occur due to two competing contributions. The contribution given by Eq. (3) causes $\rho(T)$ to go down as T is increased. In addition, we have $\Delta\rho^*(T)$, which makes a normal contribution to $\rho(T)$ which rises with increasing T. Thus at $T=T_{\min}$ both these contributions match. Therefore, for $T\sim T_{\min}$, we can write

$$\rho(T)=\rho_0-a_\rho\sqrt{T}+\Delta\rho^*(T)\ . \tag{4}$$

It is the form of $\Delta\rho^*(T)$ that now needs attention. If it is due only to electron-phonon interaction with s-d scattering, we have

$$\Delta\rho^*(T)\cong A_3T^3\ . \tag{5}$$

If it is due to electron-electron or electron-magnon scattering,

$$\Delta\rho^*(T)\cong A_2T^2\ . \tag{6}$$

In the presence of both, $\Delta\rho^*(T)$ may take the form

$$\Delta\rho^*(T)=A_2T^2+A_3T^3\ . \tag{7}$$

We fitted our data through nonlinear least-squares fit to Eq. (4) with $\Delta\rho^*(T)$ given by Eq. (7). In Fig. 8 we show some typical fits up to 50 K. [Typical fit error $(\rho_{\text{obs}}-\rho_{\text{fit}})/\rho_{\text{fit}}\sim\pm0.03\%$ As a result it is difficult to distinguish between data and fit in the figure.] The fit parameters are given in Table III. In the same table we collected the parameters obtained from data of Ref. 4 and analyzed through Eqs. (4) and (7). Parameters A_1, A_2, A_3, and a_ρ, which determine the temperature dependences, are plotted in Fig. 9. The first thing we note is

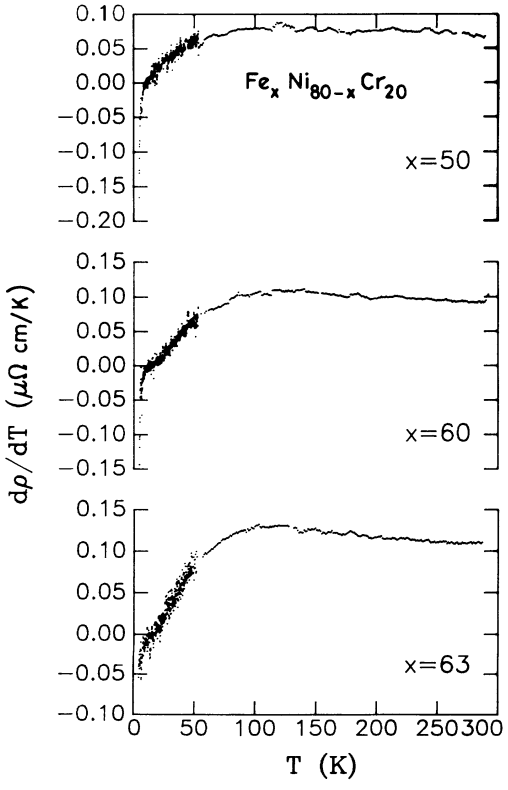

FIG. 7. Temperature dependence of resistivity derivative ($d\rho/dT$) for three representative alloys ($x=50$, 60, and 63).

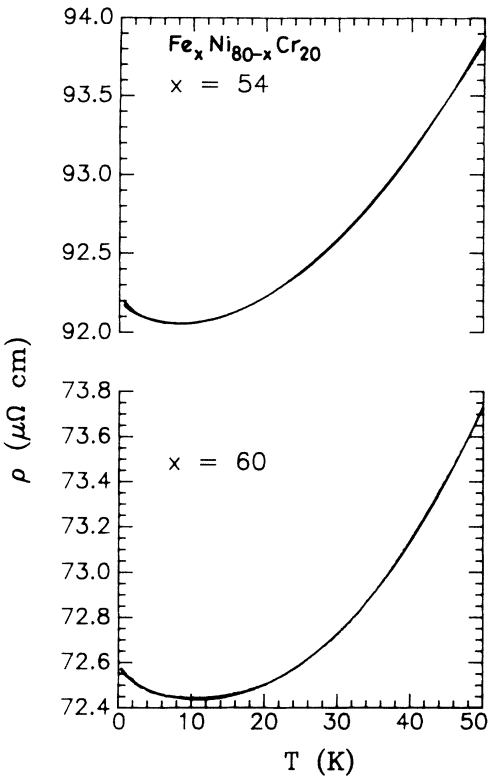

FIG. 8. Fit of $\rho(T)$ to Eqs. (4) and (7) for $T<50$ K for representative alloys. ($x=54$ and 60). The data points and fit lines are almost indistinguishable in this scale.

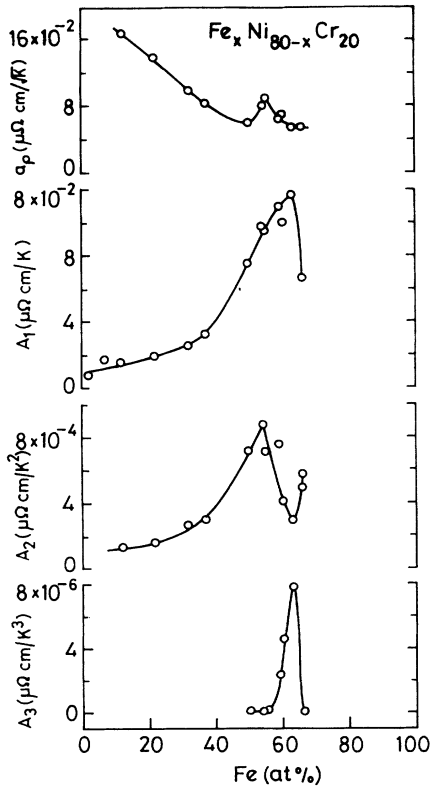

FIG. 9. Variation of the parameters a_ρ, A_2, A_3 and A_1 [Eq. (2)] which describes the temperature dependence of $\rho(T)$. For $x<37$, data of Ref. 4 have been used and reanalyzed.

that the parameters obtained from data of Ref. 4 smoothly merge with those obtained from our data. The contributions from all the terms in Eq. (4) are plotted in Fig. 10 for two samples $x=54$ and 63. It can be seen that while the sample with $x=54$ has a negligible T^3 term, there is a considerable contribution from the T^3 term (dominating above 40 K) in the alloy with $x=63$. In Fig. 4 we show the fit and data in a log scale up to 20 K, to blow up the region near T_{min} as well as the low-temperature region. It can be seen that by including the region of resistivity minima we can explain the behavior of $\rho(T)$ for 50 K $>T>0.4$ K using Eqs. (4) and (7). In Fig. 4 we observe some deviation at lower temperature for $x=50$, 54, and 66. For these compositions $\rho(T)$ has a large T^2 dependence (see Fig. 9). The significant contribution of the T^2 term causes a deviation in the fit below T_{min}. However, low-temperature fits using data only below 3 K show that $\rho(T)$ indeed has the $\sqrt{T}$-type dependence which will be

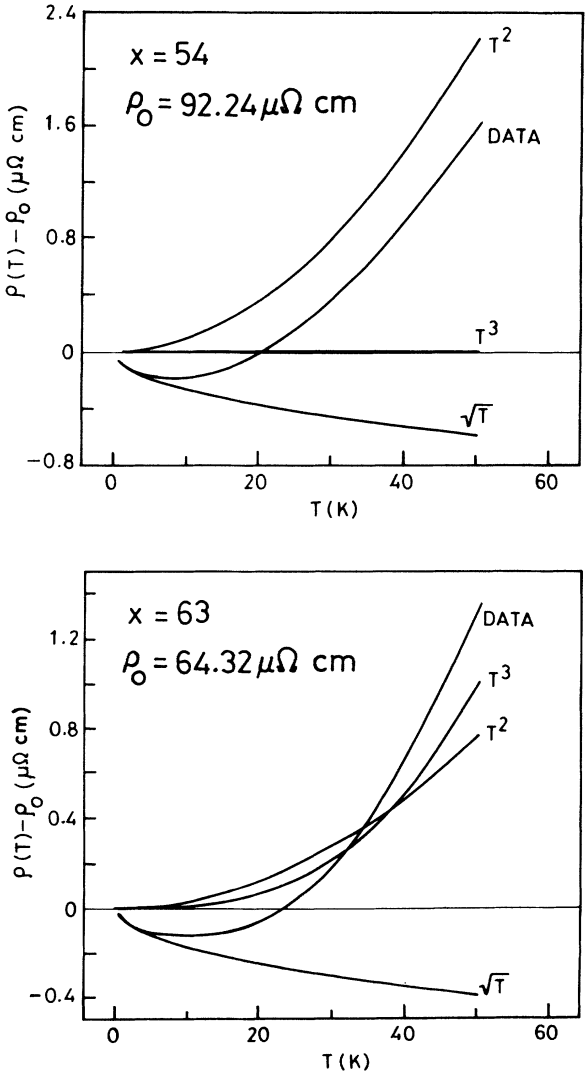

FIG. 10. A comparison of relative contributions of $\sqrt{T}$, T^2, and T^3 terms [see Eqs. (4) and (7)] for two alloys. The one with $x=63$ close to x_c has an appreciable T^3 term, while the other with $x<x_c$ has a negligible T^3 term (also see Fig. 9).

discussed in Sec. III B. (A preliminary report of the data below T_{min} has been published before.[6])

We would now like to address the issue of magnetic contribution (ρ_{mag}) to $\rho(T)$. For $T \gg T_c$, the spin disorder resistivity ρ_{mag} makes a temperature-independent contribution. The spin-disorder resistivity is expressed as[12]

$$\rho_{mag}(T \gg T_c) \propto J_{sd}^2 S(S+1) , \tag{8}$$

where S is the local magnetic moment and J_{sd} is the conduction electron-local spin interaction strength. (Whether we can use a local magnetic moment picture for these alloys is a serious issue, but for our discussion we assume that it holds.) From the measured magnetic moment (obtained from the saturation magnetization), S can be estimated. One way to establish ρ_{mag} is to look for the difference between ρ_c and ρ_0. In our case ρ_c is actually about 3 $\mu\Omega$ cm smaller than ρ_0. The determination of ρ_c from extrapolation of $\rho(T)$ at around 300 K is not error free. Because $d\rho/dT$ is slowly decreasing and has not reached a temperature-independent value at $T=300$ K, ρ_c may therefore be underestimated. In any case we do not expect an error of more than 10% in the determination of ρ_c. As a result $\rho_c \approx \rho_0$, and even if ρ_c is underestimated by 20%, $(\rho_0 - \rho_c) < 5$ $\mu\Omega$ cm. Thus we set an upper limit of $\rho_{mag} \approx 5\mu\Omega$ cm. Such a low ρ_{mag} will be difficult to detect experimentally. As a result the direct magnetic contribution to $\rho(T)$ remains unnoticed. This low value of ρ_{mag} is expected at $x \approx x_c$ because S is extremely low in these alloys close to critical concentration, and $\mu \approx 0.12\mu_B$. From a detailed investigation of different types of Ni-Fe alloys it has been found that $\rho_{mag}/S(S+1) \approx 30$ $\mu\Omega$ cm.[12] As a result, a ρ_{mag} of 5 $\mu\Omega$ cm is an extremely reasonable number for these alloys, if S is indeed small.

From the discussion above we conclude this subsection with the following remarks.

(a) At high temperature ($T > 100$ K) the resistivities are nearly linear. The high-temperature linear behavior is due to electron-phonon interaction.

(b) The resistivities near T_{min} and below 50 K contain a dominant T^2 contribution in addition to a T^3 contribution. The contribution of the T^2 term to $\rho(T)$ first increases with increasing x, and then decreases rapidly as x approaches the critical concentration x_c. There is a large increase in the contribution of the T^3 term in the critical region (see Figs. 9 and 10). We suggest that the T^3 contribution is due to electron-phonon interaction in the presence of s-d scattering. The increase in A_1 (which is also related to electron-phonon interaction) follows the same trend as A_3.

(c) The T^2 term most likely arises predominantly from spin waves. The Baber contribution, if we take a clue from pure Fe, Ni, etc., seems to be much lower than the observed T^2 contribution. The T^2 contribution as measured through A_2 increases gradually as one increases the Fe concentration. However, near the critical region it drops rather sharply (see Fig. 9). When we go to $x=66$, where we have the onset of long-range order (AFM), the A_2 term again recovers (see Fig. 9). We discuss this point in Sec. III B.

(d) The increase in A_1, A_2, A_3, etc. leads to an enhancement of $\Delta\rho(T)$ ($=\rho_{300\text{ K}} - \rho_{min}$) at the critical region (see Fig. 6), and a fall in these terms beyond $x > x_c$ gives a sharp fall in $\Delta\rho$.

(e) There is no distinct feature in $\rho(T)$ or $d\rho/dT$ at magnetic transitions. However, there is a definite systematic dependence of ρ_0 as well as different parameters (e.g., A_1, A_2, and A_3) on the composition. We will discuss this below.

(f) The upper limit on the direct magnetic contribution (ρ_{mag}) to the resistivity is estimated to be 5 $\mu\Omega$ cm.

B. Temperature dependence of resistivity for $T < T_{min}$

All the alloys of the Fe-Ni-Cr series exhibited resistivity minima except $Fe_{25}Cr_{75}$, for which a resistivity minimum was not observed down to 0.4 K. In crystalline alloys with dilute magnetic impurities (particularly 3d metals in noble metals) one often sees the existence of resistivity minima at certain temperature T_{min}; i.e., for $T < T_{min}$, $\rho(T)$ rises again following a $\ln T$ relation which is explained as due to the Kondo effect.[13] However, resistivities for the samples studied by us below T_{min} do not follow a $\ln T$ relation, generally observed for the case of dilute magnetic alloys. The resistivities at 4.2 $\sim$ K ($\rho_{4.2K}$) of the samples studied by us were of the order of 50–100 $\mu\Omega$ cm. This is evidence of a strong disorder in these alloys arising from substitutional disorder. In systems studied by us, resistivity minima occur at $T_{min} \approx 6$–11 K, and the change in $\rho(T)$ below T_{min} is very small [typically $\Delta\rho/\rho$ (0.5 K) $\approx 0.2\%$]. It is extremely difficult to determine categorically the exact nature of the temperature dependence of $\rho(T)$ unless measurements are done down to temperatures well below 4 K. We tried to fix the nature of $\rho(T)$ below T_{min} with a proper fitting procedure,[6] and found that the rise in $\rho(T)$ at low temperature follows a limiting $\sqrt{T}$-type dependence for $T < 3K < T_{min}/2$. A $\sqrt{T}$ functional dependence of $\rho(T)$ [Eq. (3)] has been observed in a number of metallic glasses[14] below 2 K. It is generally believed that this $\sqrt{T}$ dependence arises from disorder-induced electron-electron interaction.

At this point we want to present the data as conductivity (σ) rather than resistivity. To be specific, the quantum correction to the conductivity $\Delta\sigma(T)$ arising out of electron-electron interaction is given as[15,16]

$$\sigma(T) = \sigma_0 + \Delta\sigma = \sigma_0 + m\sqrt{T} , \tag{9}$$

where σ_0 is $\sigma(T=0)$:

$$m = 0.915 \left[\frac{k_B}{\hbar D}\right]^{1/2} \left[\frac{e^2}{2\pi^2\hbar}\right] \mathcal{F} \tag{10a}$$

and

$$\mathcal{F} = (\tfrac{2}{3} - \tfrac{3}{4}\tilde{F}_\sigma) . \tag{10b}$$

Here D is the electron diffusivity, and $\tilde{F}_\sigma$ is a screening constant.[14] Equations (3) and (9) are equivalent ways of writing the same thing, as long as the correction

$\Delta\sigma \ll \sigma_0$. In our case $\Delta\sigma/\sigma_0 \ll 10^{-2}$. It has been found that for most metallic glasses studied at low enough temperatures ($T < 2K$), $m \simeq 6$ S/(cm K$^{1/2}$).[14] For the alloys under consideration, $m \simeq 12-14$ S/(cm K$^{1/2}$).[6]

If the low-temperature transport in these solids (for $T < T_{\min}$) is dominated by electron-electron interactions, then the coefficient m in Eq. (9) which measures the magnitude of correction to conductivity should be a physically meaningful number. In the following we try to estimate m. The main uncertainty in the estimation of m comes from the lack of knowledge about the electron diffusivity D. Though not strictly correct,[15,16] an estimate of D can be obtained from the Einstein relation $\sigma \approx e^2 g(E_f) D$, where $g(E_f)$ is the density of states at the Fermi level E_f. Specific-heat measurements for this class of alloys (although not exactly on same compositions) show a rather large linear term in specific heat.[17,18] A typical coefficient of the linear term γ is 25 mJ/(mole/K^2). If the large linear term arises from a high $g(E_f)$ alone, this would imply that $g(E_f) \approx 5.7 \times 10^{35}$ erg^{-1} cm^{-3}. Using $\tilde{F}_\sigma \approx 0$, we then obtain $m \approx 10$ S/(cm K$^{1/2}$). Given the uncertainty in determination of D and $\tilde{F}_\sigma$, the calculated m is rather close to the experimental values. For comparison we now consider data of Ref. 4. The lowest temperature studied in Ref. 4 is 4.2 K, but $T_{\min}$ for these alloys lies around 15–35 K. Thus a reasonable estimate of m can be obtained from their data, and it is found to be ≈ 5 S/(cm K$^{1/2}$). In Table IV we collect values of m observed in a number of crystalline alloys where one sees a resistivity minima. For comparison we also show values for metallic glasses. It is quite interesting to note that for most alloys m is within a factor of 3.

We now turn our attention to the question of whether the magnetic order of the solid has any role to play in electron-electron interactions. As far as the temperature dependence of $\sigma(T)$ below $T_{\min}$ is concerned, all the alloys (FM, RSG, SG, and AFM) show a $\sqrt{T}$ dependence following Eq. (9). Thus the magnetic state of the solid does not seem to affect the temperature dependence. There is a small but systematic variation in m, and this variation is greater than the experimental uncertainties (level of uncertainty in $m \approx \pm 1\%$). It increases in the spin-glass phase and is lower both in the AFM and FM phases.[6] In fact σ_0 itself increases and follows a similar behavior. Therefore, it seems that in these alloys the effect of magnetic order, if any, on electron-electron interaction is rather small. We believe that this is the first investigation of this type of polycrystalline alloys with high concentrations of transition metals carried down to low enough temperatures that the contribution of electron-electron interaction on the transport property has been clearly identified.

To summarize this subsection, we find that the low-temperature rise in $\rho(T)$ below $T_{\min}$ arises from the quantum correction to the conductivity due to electron-electron interactions, and has a $\sqrt{T}$-type temperature dependence. We also find that this $\sqrt{T}$ behavior does not have any strong dependence on the magnetic state of the alloy. However, for concentration regions where there is no long-range magnetic order, we find a slight enhancement of the quantum correction to conductivity as measured by m. The value of m is similar (within a factor of 3) in a large number of metallic alloys where a $\sqrt{T}$ rise in $\rho(T)$ at low temperature has been observed.

TABLE IV. Observed value of m for some alloys where one sees a resistivity minima.

Sample	Reference	ρ ($\mu\Omega$ cm)	m [S/(cm K$^{1/2}$)]
$Pd_{82}Cr_{18}$	14	64	4.8
$Fe_{58.37}Ni_{31.43}Mn_{10.2}$	21	110	15.0
$Fe_{12}Ni_{68}Cr_{60}$	4	100	8.9
$Fe_{60}Ni_{20}Cr_{20}$	6	98	14.0
Amorphous alloys	14	105–175	3.7–7
$Fe_xNi_{80-x}Si_8B_{12}$ [a]	14	105–109	5.6–8.4

[a] $x \leq 10.4$ amorphous alloy.

C. Resistivity of $Fe_{25}Cr_{75}$

Magnetic properties of Fe_xCr_{100-x} (Ref. 19) for $20 \leq x \leq 30$ at low temperature ($T \leq 30$ K) reveals a complex magnetic behavior quite similar to the Fe-Ni-Cr series. For the purpose of this work such details are not important. Fe-Cr forms a bcc alloy in this composition range and is thus distinct from γ-phase Fe-Ni-Cr alloys, although both alloys are highly resistive and have complex magnetic phases near the critical composition for ferromagnetism. The reason for studying the Fe-Cr alloy is to produce reference data for the α-phase alloy, with which we can compare and contrast the data for γ-phase alloys.

$Fe_{25}Cr_{75}$ undergoes PM-FM transition at $T_c \sim 150$ K and FM-ASM (ASM: asperomagnet) a transition at $T_{\rm ASM} \sim 20$ K. As in the Fe-Ni-Cr system, the $\rho(T)$ of these alloys does not show any features at T_c or $T_{\rm ASM}$ either in $\rho(T)$ (Fig. 5) or $d\rho/dT$ (Fig. 11). However, as pointed out above, this system does not show a resisitivi-

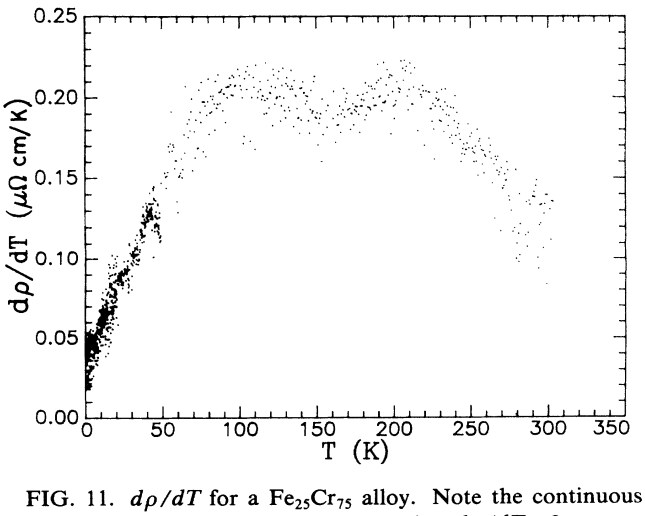

FIG. 11. $d\rho/dT$ for a $Fe_{25}Cr_{75}$ alloy. Note the continuous decrease of $d\rho/dT$ for $T > 200$ K, and that $d\rho/dT > 0$ even at the lowest temperatures.

ty minimum down to 0.4 K (see Fig. 5), even though the room-temperature resistivity ($\rho_{300\,K} \sim 104$ $\mu\Omega$ cm) is comparable to those in the Fe-Ni-Cr series (90–120 $\mu\Omega$ cm). The resistivity of this alloy continues to drop as the temperature is reduced to 0.4 K, showing no sign of saturation (even at 0.4 K $d\rho/dT$ is finite and positive; see Fig. 11). This behavior is in sharp contrast to that observed in the Fe-Ni-Cr series. This observation, in our opinion, is extremely important. This shows that high resistivity (hence low D) alone is not the criterion for an observation of resistivity minima. The resistivity minima will be absent, or occur at $T \ll 0.4$ K if m is very small. This happens when $\tilde{F}_\sigma$ is such that two terms in Eq. 10(b) are almost balanced.

At higher temperatures $\rho(T)$ for this alloy has a sigmoidal shape, as shown in Fig. 5. $\rho(T)$ follows a T^2 dependence for $T \leq 80$ K, a linear T dependence in the temperature range 100–200 K, and a large negative deviation from linearity above 200 K which shows an approach to resistivity saturation (see Fig. 5). Such a distinct sigmoidal shape is definitely absent in γ-phase alloys at 300 K. The $d\rho/dT$ vs T shown in Fig. 11 clearly indicates resistivity saturation ($T \geq 300$ K), because $d\rho/dT$ continues to drop as T is increased even near the room temperature. There is a split peak around 150 K. We do not know the origin of this. The coefficients of the high-temperature (approximate) linear T dependence (19.60×10^{-2} $\mu\Omega$ cm/K) and the low-temperature quadratic T^2 dependence (1.819×10^{-3} $\mu\Omega$ cm/K^2) are found to be more than twice the coefficients A_1 and A_2, respectively, obtained for the Fe-Ni-Cr series (see Table III). These large A_1 and A_2 give a large $\Delta\rho$ ($\simeq 53 \mu\Omega$ cm) for this alloy.

From the deviation of $\rho(T)$ from linearity, we can find $\rho_{sat} \simeq 350$ $\mu\Omega$ cm (ρ_{sat} is the saturation value of ρ at higher temperature; see Ref. 11 for the procedure for obtaining ρ_{sat}). ρ_{sat} is almost the same as the Ioffe-Regel resistivity ρ_{IR} ($=\hbar a/e^2$; a is the lattice constant). For this alloy $a = 2.87$ Å and $\rho_{IR} = 354$ $\mu\Omega$ cm. For fcc Fe-Ni-Cr alloys, $a = 3.60$ Å and $\rho_{IR} = 440$ $\mu\Omega$ cm, which is higher than that of the Fe-Cr alloy. Thus $\rho(T)$ for Fe-Ni-Cr alloys has to grow more [$\simeq 140$–150 $\mu\Omega$ cm] before we see any effect of ρ_{sat} on $\rho(T)$. This should therefore occur at high temperatures, if it occurs at all.

Below we summarize the principal observation of this subsection.

(i) The main difference seems to be the presence of a minima in $\rho(T)$ of γ-phase iron alloys for the whole composition range, while for the α-phase alloy (lying close to the critical composition) one does not find any minima in ρ. Such a minima also has been seen in Fe-Ni-Mn alloys.[20] It may be that the presence of Ni causes this difference in these alloys, or it may be a property of γ-phase alloys.

(ii) At high temperature in Fe-Ni-Cr alloys $\rho \propto T$, with no sign of an approach to resistivity saturation at $T = 300$ K. However in the Fe-Cr alloy, ρ shows a sigmoidal shape with a distinct trend toward saturation at high temperature. This difference arises due to a lower ρ_{IR} in the Fe-Cr alloy.

IV. COMPOSITION DEPENDENCE OF RESISTIVITY AND RELATED PARAMETERS

In this section we will discuss the evolution of the resistivity behavior in this alloy series as we go from the Ni-rich (small x) to Fe-rich (large x) ends through the critical region where one observes distinct features. Resistivities in these alloys as we saw above, receive very little direct contribution from magnetism through spin-disorder scattering. Nevertheless, we see clear features in resistivities at and near the critical concentration ($59 \leq x \leq 63$). We will show below that there seems to be a direct connection to the occurrence of these features near the critical region and the absence of long-range magnetic order (or the presence of magnetic disorder). This shows up mainly through the collapse of the magnetic moment, the decrease of the spin-wave stiffness constant and strength of the s-d scattering, and the cessation of the spin wave as a propagating excitation in the critical region of phase diagram.

The first thing to note is that the residual resistivity (ρ_o) evolves continuously as x is changed, but that there are two distinct regions. In the Ni-rich end ($x \leq 40$), $\rho_0 \approx 100 \pm 5$ $\mu\Omega$ cm. However, in the Fe-rich end ρ_0 starts to drop and falls rather rapidly for $x > 54$, and reaches a minimum of $\rho_0 \simeq 60$ $\mu\Omega$ cm at $x = 63$. In the AFM phase ρ_0 shows a slight recovery. In this Fe-rich end, close to the critical region, the value of ρ_0 is very similar to that for 304 stainless steel. (To be specific, for $Fe_{64}Ni_{20}Cr_{16}$ $\rho_0 \approx 55$ $\mu\Omega$ cm, and for $Fe_{59}Ni_{25}Cr_{16}$, $\rho_0 \approx 64$ $\mu\Omega$ cm.[21]) In the Ni-rich end, for $x = 0$ we start with paramagnetic fcc alloy $Ni_{80}Cr_{20}$ with $\rho_0 = 100$ $\mu\Omega$ cm. The high value of ρ_0 in this alloy arises due to Cr, which forms a virtual bound state (VBS) near the Fermi level.[22] Using the language of the "two-current model," the formation of VBS on Cr addition gives $\rho_{0\uparrow} \approx 16$ $\mu\Omega$ cm/at. %, $\rho_{0\downarrow} \approx 7.2$ $\mu\Omega$ cm/at. %, and $\rho_0 \approx 5$ $\mu\Omega$ cm/at. % Cr ($\rho_{0\sigma}$ is the residual resistivity due to σ spin band), and this saturates only beyond 20 at. % Cr. As x is increased from zero by adding Fe in place of Ni, we have a slight increase of ρ_0 to around 105 $\mu\Omega$ cm for $x \simeq 25$. In this region the matrix is predominantly Ni, and addition of Fe is similar to what happens in the Ni-Fe alloy.[23] $Ni_{100-x}Fe_x$ retains its fcc structure for $x < 65$, and in the region $x < 40$ ρ_0 saturates to a value of around 5 $\mu\Omega$ cm. The increase in ρ_0 of the $Ni_{80-x}Fe_xCr_{20}$ to around 105 $\mu\Omega$ cm for $x \simeq 25$ (from $\rho_0 \simeq 100$ $\mu\Omega$ cm for $x = 0$) is thus understandable. In this region both T_c as well as the magnetic moment μ (derived from saturation magnetization) increase as x is increased.[3] The rise most likely arises from Fe spins, but concentration of Fe being low, antiferromagnetic Fe-Fe interaction (expected in γ-Fe) has not yet set in.

In the Fe-rich end the limiting composition is $Fe_{80}Cr_{20}$. From previous studies[24] of both Cr-rich and Fe-rich Fe-Cr alloys, and our studies of the $Fe_{25}Cr_{75}$ alloy, we estimate that $Fe_{80}Cr_{20}$ should have a value of $\rho_0 \approx 50$–60 $\mu\Omega$ cm. (When Cr is added to Fe, $\rho_0 \simeq 2.6$ $\mu\Omega$ cm/at. % Cr.) For $x \geq 25$ the Cr finds itself increasingly in an Fe environment, and eventually the alloy appears similar to a Fe-Cr binary doped with Ni. It is thus expected that

ρ_0 in the Fe-rich end will have a smooth decrease to the ρ_0 value of $Fe_{80}Cr_{20}$. In Fig. 6, we have shown by a dashed line how ρ_0 "should" decrease monotonically for $25 \leq x \leq 80$ if there was no anomaly at $x \approx x_c$. Barring the critical $(54 \leq x \leq 66)$ region, we can say that ρ_0 evolves smoothly from a ρ_0 of $Ni_{80}Cr_{20}$ to a ρ_0 of $Fe_{80}Cr_{20}$ as x increases, and the high resistivity for these alloys arises due to Cr, which is known to form VBS at the Fermi level in both Ni and Fe.[23]

We would now like to address the anomalous behavior of ρ_0 around the critical region. This drop in resistivity can be caused by a rather sharp drop in $g(E_f)$, implying that we have less d-type states to scatter to. However, the experimental determination of γ (the coefficient of linear specific heat) in alloys of similar composition show a rise in γ near the critical region. However, this contradicts what is observed, and calls for a somewhat critical analysis of the situation. If both spin-up and spin-down d bands are occupied, then an enhancement of γ will not lead to extra ρ_0. This is quite likely because our magnetoresistance measurement at 4.2 K showed extremely small (or negligible) ferromagnetic anisotropy,[25] implying equal population of spin-up and spin-down bands. The increase of γ in this region may also completely arise from a magnetic contribution.[7] If so, then the fall in ρ_0 at $x \approx x_c$ will not be related to γ. It can also mean that additional states at E_f contributing to γ have a predominantly s character, and they can lead to enhanced charge-carrier concentration and a decrease in ρ_0. This is what we think we observed in our Hall measurement (see Fig. 12), keeping in mind the caution that the Hall concentration may not represent the true carrier concentration. If this is indeed an enhancement of the mobile carrier concentration (as seen in Fig. 12), a drop in ρ_0 in this region as well as its recovery beyond the critical region can be explained. It is thus plausible that the anomalous behavior of ρ_0 near the critical region is a reflection of enhancement of the charge-carrier concentration. Note: Measurement of R_H has been done in a field of 1.8 T at room temperature, which is much larger than the highest T_c ($\simeq 120$ K) of the alloys. This was done to avoid any contribution from the extraordinary Hall effect. However, we understand the limitations of such a Hall measurement, and exercise caution not to extract too much information from it. It may also be noted that we have a positive R_H.)

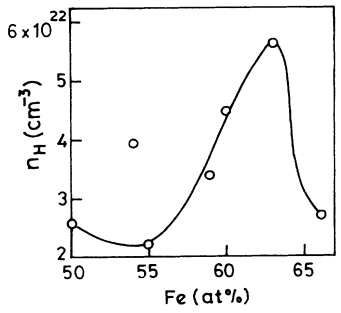

FIG. 12. Hall concentration n_H $(=R_H^{-1})$ as a function of x. R_H has been measured at 300 K for field of 1.8 T.

The temperature-dependent part of the resistivity, represented by $\Delta\rho(\rho_{300\text{ K}}-\rho_{\min})$, shows a peak in the critical region $x \simeq 59-63$. It starts rising from $x \simeq 37$, and after passing through a maximum at the critical region it falls again. This behavior of $\Delta\rho$ when added to ρ_0 $(\simeq\rho_{\min})$ produces the sharp peak in $\rho_{300\text{ K}}$ for $x \simeq 54$ (see Fig. 6). $\Delta\rho$ consists of T^2 and T^3 terms at low temperature, and a linear term at higher temperatures [see Eqs. (7) and (2)] which are represented by coefficients A_2, A_3, and A_1, respectively. The variation in A_1, A_2, and A_3 reflect the variation in $\Delta\rho$ (see Figs. 6 and 9). A_1 rises continuously as Fe is added in place of Ni, and shows a peak at $x=63$. A_2 rises and shows a peak at $x \simeq 54$, falls to a minimum at $x \simeq 63$, and recovers at $x \simeq 66$. A_3 is extremely small far away from the critical region, and it shows a peak at $x \simeq 63$.

Our explanation for A_2 is that it arises from electron-magnon scattering, and is given by[26]

$$A_2 \propto SG/D_{\text{sw}}^2 , \tag{11}$$

where S is the spin, G is the coupling constant of the spin wave to electrons and D_{sw} is the spin-wave stiffness constant. The A_2 term in the Ni-rich end approaches a limiting of 0.1 $n\Omega$ cm/K^2 and its maximum value at $x=54$. As Fe is substituted for Ni, neutron-scattering data[3] show that the spin-wave stiffness constant D_{sw} goes down almost linearly (for $x \geq 40$), and that it lies between 150 and 20 meV Å^2. The spin S also goes down somewhat for $40 \leq x \leq 75$, as inferred from the magnetic moment μ obtained from the saturation magnetization data.[3] However, since D_{sw} goes down more rapidly as x is increased, and appears as D_{sw}^2 in the denominator, A_2 increases rather rapidly in the region $40 \leq x \leq 54$. In this region, our data confirm neutron-scattering data showing that well-defined spin waves exist in these alloys and that they scatter electrons.

The drop of A_2 for $x > 54$ is due either to the collapse of the magnetic moment on approaching the critical region, or to the fact that the spin wave in this region does not exist as a well-defined propagating excitation. Neutron-scattering experiments done in a similar region for the Fe-Cr alloy show that the spin-wave energy decreases continuously, and that the damping increases as the critical region is approached.[27] The recovery of A_2 in the antiferromagnetic region is possible if the antiferromagnetic spin wave is established in this region of long-range order. The fact that the rise in A_2 is linked to a softening of the spin-wave stiffness constant can be seen for the alloy $Fe_{25}Cr_{75}$. In this alloy $A_2 \simeq 1.8$ $n\Omega$ cm/K^2. This is a factor of 2 higher than the highest A_2 $(=0.9$ $n\Omega$ cm/K$^2)$ observed in the Fe-Ni-Cr series. D_{sw} for $Fe_{25}Cr_{75}$ as measured from neutron-scattering experiments[27] is $\cong 15$ meV/Å^2. It is therefore expected that A_2 will be much higher for the $Fe_{25}Cr_{75}$ alloy if other factors are not too different. We thus conclude that the T^2 term is a signature of electron-magnon scattering. The drop of A_2 at the critical region is due to the collapse of the spin wave as well-defined excitation, or a collapse in S (or both), and the initial rise in the ferromagnetic region (for

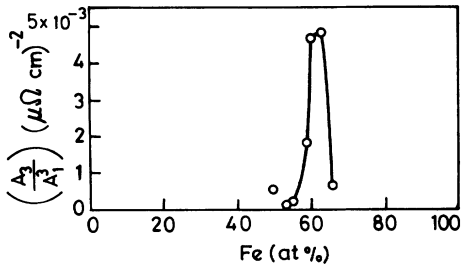

FIG. 13. A_3/A_1^3 as a function of x.

$20 \leq x \leq 54$) is due to softening of the spin-wave stiffness constant.

The rises in A_1 and A_3 (as x is varied) are linked together if they arise from a Bloch-Wilson-type of electron-phonon interaction (including s-d scattering). In that case $A_1 \propto K_{sd}/\theta_{sd}$ and $A_3 \propto K_{sd}/\theta_{sd}^3$, where K_{sd} is the electron-phonon coupling constant in the presence of s-d scattering. The rise in A_1 and A_3 as the critical region is approached can come from a decrease in θ_{sd} and/or a rise in K_{sd}. To check this, we consider the quantity A_3/A_1^3, which is independent of θ_{sd} and $\propto 1/K_{sd}^2$. If K_{sd} remains constant as x is varied, A_3/A_1^3 should also remain constant. In Fig. 13 we show A_3/A_1^3 as a function of x. We find that A_3/A_1^3 has a sharp maximum at $x = 60-63$, the critical region. This implies that K_{sd} actually decreases in this region. Therefore, the gradual increase in A_1 and A_3 as x is increased arises from a decrease of θ_{sd}. This decrease of θ_{sd} actually offsets the decrease in A_1 and A_3 arising from the decrease in K_{sd}. On further increase of x (i.e., in the AFM phase), one finds A_3/A_1^3 and hence K_{sd} has increased to its normal value. K_{sd} is linked to the strength of s-d scattering as well as to the charge-carrier concentration. The decrease in K_{sd} near the critical region would mean a decrease in the s-d scattering. (This is the same conclusion we obtained previously from analysis of ρ_0 and/or an increase in carrier concentration.)

In the above analysis, we have tried (in a qualitative fashion) to explain the composition dependence of the observed resistivity data. We have also tried to establish links with various other properties of the material, in particular with the nature of the critical region. It will be interesting to make similar studies of systems like Fe-Ni-Mn, and to check the validity of some of the explanations offered here.

V. SUMMARY AND CONCLUSION

In this paper we presented an extensive study of the resistivity of Fe-Ni-Cr alloys for almost the entire region of composition where Fe preserves the γ phase for a given Cr concentration. A number of interesting behaviors were observed. In particular, there are distinct features in resistivities for alloys lying close to the critical region. We tried to provide a qualitative and semiquantitative explanations for the observed behavior. Though the direct contribution from the magnetic contribution to $\rho(T)$ seems to be quite low, the indirect contribution of the magnetic order (or its absence) in the critical region is clearly seen in the resistivity.

Below we summarize the answers to the questions raised in Sec. I.

(a) The high resistivity (ρ_0) of these alloys arises from the presence of Cr, which forms VBS near the Fermi level. (Cr is known to form VBS when added to either Ni or Fe.) The change in ρ_0 from 100 $\mu\Omega$ cm for the Ni-rich end (low x) to ~ 60 $\mu\Omega$ cm for the Fe-rich end (high x) arises because Cr finds itself in a predominantly Ni (Fe) environment for low (high) x.

(b) With concentrated magnetic constituents, we are not in the traditional Kondo regime. There does exist a resistivity minima at low temperature in Fe-Ni-Cr alloys, although it arises from origins not related to the Kondo effect.

(c) For alloys lying close to the critical region, the direct magnetic contribution to ρ_0 can be quite small, because the average moment μ leading to the magnetic contribution is very small. Also, any feature in $\rho(T)$ or $d\rho/dT$ at $T \simeq T_c$ may not be possible to observe. However, near the critical region features such as vanishing of $\bar{\mu}$, change in the spin-wave stiffness constant, and other related factors contribute to $\Delta\rho(T)$, and give rise to rather interesting variations as x is changed.

(d) The absence of the spin wave as a propagating exciton near the critical region (SG and RSG phases) shows up in the rapid decrease of the T^2 term in $\rho(T)$ (which arises from electron–spin-wave scattering) in the region $59 \leq x \leq 63$.

(e) There are important quantitative as well as qualitative differences between Fe-Ni-Cr alloys and the Fe-Cr alloy. In the first case we find well-defined resistivity minima. These are present in at least one other γ-phase Fe alloy Fe-Ni-Mn. At the high-temperature end at 300 K, we see no approach to resistivity saturation for Fe-Ni-Cr alloys, but $Fe_{25}Cr_{75}$ shows a clear approach to saturation even at 300 K. This difference most likely arises from the difference in ρ_{IR}, which is smaller for $Fe_{25}Cr_{75}$ because of the smaller lattice spacing (α-Fe structure).

(f) Qauntum interference effects (electron-electron interaction), which give rise to a $\sqrt{T}$ correction to conductivity, can explain the existence of resistivity minima in these alloys. The onset of long-range magnetic order (or its absence) seems not to have much effect on this correction.

ACKNOWLEDGMENTS

The authors want to thank Professor A. K. Majumdar of IIT/Kanpur for supplying some of the samples, and CSIR for financial support through a sponsored project.

[1]J. S. Dugdale, Contemp. Phys. **28**, 547 (1987).
[2]A. K. Majumdar and P. v. Blankenhagen, Phys. Rev. B **29**, 4079 (1984).
[3]A. Z. Men'shikov and A. Ye. Teplykhi, Fiz. Met. Metalloved. **44**, 1215 (1977) [Phys. Met. Metallogr. **44**, 78 (1979)]; A. Z. Men'shikov, N. N. Kuz'min, V. N. Kazantev, S. K. Sidorov, and A. N. Kalinin, *ibid.* **40**, 647 (1975) [*ibid.* **40**, 174 (1975)].
[4]A. V. Butenko, D. N. Bol'shutkin, and V. I. Pecherskaya, Zh. Eksp. Teor. Fiz. **98**, 1752 (1990) [Sov. Phys. JETP **71**, 983 (1990)]; V. I. Pecherskaya, A. V. Butenko, and A. I. Kopeliovich, Fiz. Nizk. Temp. **16**, 267 (1990) [Sov. J. Low Temp. Phys. **16**, 149 (1990)]; V. I. Pecherskaya, A. V. Butenko, and D. N. Bol'shutkin, *ibid.* **15**, 952 (1989) [*ibid.* **15**, 525 (1989)].
[5]S. B. Roy, A. K. Majumdar, N. C. Mishra, A. K. Raychaudhuri, and R. Srinivasan, Phys. Rev. B **31**, 7458 (1985).
[6]S. Banerjee and A. K. Raychaudhuri, Solid State Commun. **83**, 1047 (1992).
[7]E. F. Wassermann, Adv. Solid State Phys. **27**, 85 (1987); E. F. Wassermann, Phys. Scr. **T25**, 209 (1989).
[8]A. Z. Menshikov, J. Magn. Magn. Mater. **10**, 205 (1979).
[9]S. Banerjee, Ph.D. thesis, IISc Bangalore, 1993.
[10]R. Canton and R. Viswanathan, Phys. Rev. B **25**, 179 (1982).
[11]H. Wiesmann, M. Gurvitch, H. Lutz, A. Ghosh, B. Schwarz, M. Strongin, P. B. Allen, and J. W. Halley, Phys. Rev. Lett. **38**, 782 (1977).
[12]R. J. Weiss and A. S. Marotta, J. Phys. Chem. Solids **9**, 302 (1959).
[13]A. J. Heeger, *Solid State Physics-Advances in Research and Application,* edited by F Seitz, D. Turnbull, and H. Ehrenreich (Academic, New York, 1961), Vol. 23, p. 283.
[14]R. W. Cochrane and J. O. Strom-Olsen, Phys. Rev. B **29**, 1088 (1984); **43**, 6042 (1991); G. Thumes, J. Kötzler, R. Ranganathan, and R. Krishnan, Z. Phys. B **69**, 489 (1988).
[15]P. A. Lee and T. V. Ramakrishnan, Rev. Mod. Phys. **57**, 287 (1985).
[16]B. L. Altshuler and A. G. Aronov, *Electron-electron Interaction in Disordered Systems,* edited by A. L. Efros and M. Pollak (North-Holland, Amsterdam, 1985), pp. 4–153.
[17]V. I. Pecherskaya, D. N. Bol'shutkin, A. V. Butenko, V. N. Bellinson, V. I. Ovcharenko, V. A. Pervakov, and N. Yu. Tyutryumova, Fiz. Nizk. Temp. **14**, 919 (1988) [Sov. J. Low Temp. Phys. **14**, 505 (1988)].
[18]W. Bendick and W. Pepperhoff, J. Phys. F **11**, 57 (1981).
[19]V. I. Anisomov, V. G. Vaks, and G. A. Susloparov, Fiz. Tverd. Tela (Leningrad) **32**, 918 (1990) [Sov. Phys. Solid State **32**, 542 (1990)].
[20]Ch. Böttger and J. Hesse, Z. Phys. B **75**, 485 (1989).
[21]*CRC Handbook of Chemistry and Physics,* 74th ed., edited by David R. Lide (CRC, Boca Raton, FL, 1993), pp. 12–160.
[22]A. Fret and I. A. Campbell, J. Phys. F **6**, 849 (1976); O. Jaoul, I. A. Campbell, and A. Fret, J. Magn. Magn. Mater **5**, 23 (1977).
[23]M. C. Cadeville and B. Loegel, J. Phys. F **3**, L115 (1973).
[24]F. T. Hedgcock, J. O. Strom-Olsen, and D. F. Wilford, J. Phys. F **7**, 855 (1977).
[25]S. Banerjee and A. K. Raychaudhuri, J. Phys. Condens. Matter **5**, L295 (1993).
[26]T. Kasuya, Prog. Theor. Phys. **22**, 227 (1959); I. Mannari, *ibid.* **22**, 335 (1959).
[27]S. M. Shapiro, C. R. Fincher, A. C. Palumbo, and R. D. Parks, Phys. Rev. B **24**, 6661 (1981).